Journal of Neurochemistry

JOURNAL OF NEUROCHEMISTRY | 2010 | 114 | 886–896 doi: 10.1111/j.1471-4159.2010.06820.x

Carboxypeptidase E cytoplasmic tail mediates localization of synaptic vesicles to the pre-active zone in hypothalamic pre-synaptic terminals

Hong Lou,*,[1] Joshua J. Park,*,†,[1] Niamh X. Cawley,* Annahita Sarcon,* Lei Sun,‡ Tiffany Adams* and Yoke Peng Loh*

*Section on Cellular Neurobiology, Program on Developmental Neuroscience, Eunice Kennedy Shriver National Institute of Child Health and Human Development, National Institutes of Health, Bethesda, Maryland, USA

†Department of Neurosciences, University of Toledo, School of Medicine, Toledo, Ohio, USA

‡Department of Pharmacology, University of Michigan, School of Medicine, Ann Arbor, Michigan, USA

Abstract

How synaptic vesicles (SVs) are localized to the pre-active zone (5–200 nm beneath the active zone) in the nerve terminal, which may represent the slow response SV pool, is not fully understood. Electron microscopy revealed the number of SVs located in the pre-active zone, was significantly decreased in hypothalamic neurons of carboxypeptidase E knockout (CPE-KO) mice compared with wild-type mice. Additionally, we found K^+-stimulated glutamate secretion from hypothalamic embryonic neurons was impaired in CPE-KO mice. Biochemical studies indicate that SVs from the hypothalamus of wild-type mice and synaptic-like microvesicles from PC12 cells contain a transmembrane form of CPE, with a cytoplasmic tail (CPE_{C10}), maybe involved in synaptic function. Yeast two-hybrid and pull-down experiments showed that the CPE cytoplasmic tail interacted with γ-adducin, which binds actin enriched at the nerve terminal. Total internal reflective fluorescence (TIRF) microscopy using PC12 cells as a model showed that expression of GFP-CPE_{C15} reduced the steady-state level of synaptophysin-mRFP containing synaptic-like microvesicles accumulated in the area within 200 nm from the sub-plasma membrane (TIRF zone). Our findings identify the CPE cytoplasmic tail, as a new mediator for the localization of SVs in the actin-rich pre-active zone in hypothalamic neurons and the TIRF zone of PC12 cells.

Keywords: actin cortex, carboxypeptidase E, glutamate secretion, hypothalamic neuron, PC12 cells, γ-adducin.

J. Neurochem. (2010) **114**, 886–896.

Synaptic vesicle components, including vesicular membrane proteins, are constantly transported by constitutive vesicles from the cell soma to the active zone at the pre-synaptic membrane. Synaptic vesicles (SVs) are formed by recycling from the pre-synaptic plasma membrane, filled with neurotransmitters and held in the nerve terminal in an actin-dependent manner (Murthy and De Camilli 2003; Siksou *et al.* 2007).

In nerve terminals, there are three different synaptic vesicle pools with respect to their sensitivity to stimulation (Rizzoli and Betz 2005): a reserve pool (~80% of the pre-SVs) that responds to stimulation very slowly (~min), a slow response pool (~19%) that secretes neurotransmitters more acutely (within a few seconds), and a readily releasable pool of SVs that are docked to the pre-synaptic membrane at the active zone (~1%), and responds immediately to stimulation. Upon extracellular stimulation, the readily releasable pool is fused to the plasma membrane by Soluble N-ethylmaleimide-sensitive factor Attachment Protein Receptors and releases its neurotransmitters to the synaptic cleft. To refill the readily releasable pool depleted after exocytosis during stimulation,

Received April 14, 2010; revised manuscript received May 7, 2010; accepted May 9, 2010.

Address correspondence and reprint requests to Y. Peng Loh, National Institute of Health, Bldg 49, Rm 5A22, 49 Convent Drive, Bethesda, MD 20892, USA. E-mail: lohp@mail.nih.gov

[1]Both authors contributed equally to this work.

Abbreviations used: CPE_{C25}, C-terminal 25 amino acids of CPE; CPE-KO, carboxypeptidase E knockout; EM, electron microscopy; GFP, green fluorescent protein; GST, glutathione-*S*-transferase; I-CPE, internal sequence of CPE; LDCV, large dense-core vesicle; mRFP, monomeric red fluorescent protein; SLMV, synaptic-like microvesicles; SVs, synaptic vesicles; Syn, synaptophysin; TGN, *trans*-Golgi network; TIRF, total internal reflective fluorescence; VAMP 2, vesicle-associated membrane protein 2; VGLUT, vesicular glutamate transporter; WT, wild-type.

sufficient SVs should be available in the slow response and reserve pools within the pre-active zone, a region proximal to the active zone (Murthy and De Camilli 2003). Synapsin, an F-actin interacting protein has recently been shown to structurally maintain the SVs within the pre-active zone (Bloom *et al.* 2003; Siksou *et al.* 2007), and scaffolding proteins, including Rim1, have also been reported to contribute to the maintenance of SVs in these zones (Wang *et al.* 1997; Dieck *et al.* 1998; Fenster *et al.* 2000).

Carboxypeptidase E (CPE) is a major component in large dense-core vesicles (LDCVs) in neuroendocrine cells and exists in both soluble and membrane forms (Fricker *et al.* 1990; Dhanvantari *et al.* 2002). The soluble form of CPE within the lumen of the LDCV removes basic residues from the C-terminus of endoproteolytically cleaved proneuropeptides to yield biologically active peptides (Fricker and Snyder 1982). A luminal domain of the membrane form of CPE can bind brain-derived neurotrophic factor (Lou *et al.* 2005) and proopiomelanocortin (Cool *et al.* 1997) at the *trans*-Golgi network (TGN) and facilitate sorting of these molecules into vesicles of the regulated secretory pathway in hippocampal neurons and pituitary cells, respectively. Furthermore, a portion of the membrane-associated CPE acquires a transmembrane orientation at the TGN (pH 6.0∼6.5) and exposes its C-terminal 10 amino acids to the cytoplasm to form a cytoplasmic tail (Dhanvantari *et al.* 2002). In hippocampal neurons and anterior pituitary cells, the CPE cytoplasmic tail mediates the transport of brain-derived neurotrophic factor- and proopiomelanocortin-containing vesicles to the secretion sites via its interaction with microtubule motor complex proteins, dynactin and kinesin 2 and 3 (Park *et al.* 2008a,b). Additionally, CPE-KO mice showed impaired glutamate neurotransmission as evidenced by the lack of glutamate-mediated b-wave in their retinograms (Zhu *et al.* 2005) and deletion of the *Caenorhabditis elegans* CPE ortholog, *egl-21*, impaired the secretion of acetylcholine from the neuromuscular junction (Jacob and Kaplan 2003). Both results strongly indicate that CPE plays some role in neurotransmitter secretion.

Based on these observations, we searched for a physiological link between CPE and neurotransmitter secretion using hypothalamic neurons which we found had SVs enriched in CPE, and PC12 cells which contain acetylcholine synaptic-like microvesicles (SLMVs) and CPE. This study demonstrates that some of the CPE present in hypothalamic SVs and SLMVs have a transmembrane orientation and a cytoplasmic tail. The cytoplasmic tail interacts directly with γ-adducin, an F-actin interacting protein (Li *et al.* 1995; Takei *et al.* 1995). Glutamate release was impaired and the number of SVs in the pre-active zone of hypothalamic neurons was significantly reduced in the CPE-KO mice. Finally, competition studies *in vivo* with the CPE cytoplasmic tail eliminated SLMV accumulation in the total internal reflective fluorescence (TIRF) zone within 200 nm from the plasma membrane of PC12 cells, indicating a role of CPE in neurotransmitter release.

Materials and methods

DNA constructs

To generate the glutathione-*S*-transferase (GST)-tagged CPE_{C10} cytoplasmic tail construct, 5′-*Eco*RI–*Xho*I-3′ digests of PCR products for CPE_{C10} were subcloned into pGEX4T-2 vector (Amersham Pharmacia Biotech, Piscataway, NJ, USA). For the green fluorescent protein (GFP)-CPE_{C15} construct, CPE_{C15} was cloned into the C-terminal end of GFP in the pEGFP-3C vector (BD Bioscience, San Jose, CA, USA) at the 5′-*Eco*RI–*Kpn*I-3′ sites. Synaptophysin-monomeric red fluorescent protein (mRFP) (Syn-mRFP) was a gift from Dr Leon Lagnado (Cambridge, UK).

Secretion analysis of embryonic hypothalamic neuron and adult synaptosomes

Embryonic hypothalamic neurons isolated from an entire litter at E16 derived from mating two heterozygote ($Cpe^{+/-}$) mice as described earlier (Lou *et al.* 2005) with modification. Briefly, the hypothalamus from each embryo was dissociated individually with digestion buffer (15 mg collagenase, 5 mg DNase, 40 mg of bovine serum albumin in 10 mL phosphate-buffered saline) at 37°C for 30 min, and grown in a collagen coated 12-well plate. The genotype was identified by PCR of genomic DNA isolated from the embryo as described previously (Cawley *et al.* 2004). After 8 days, the neurons were harvested to assess the total glutamate content from the CPE-KO mice ($N = 2$) and their wild-type (WT) littermates ($N = 3$), and a total of 20 neuron cultures from CPE-KO or WT mice were subjected to an activity-dependent secretion study as described as previously with modification (Lou *et al.* 2007). The neurons were washed and equilibrated with 500 μL of basal buffer for 1 h, and then incubated with 200 μL of fresh basal buffer for 10 min for basal secretion, followed by 10 min incubation with 200 μL of 50 mM KCl-containing buffer for stimulated secretion. The samples of total cells and basal or stimulation buffer were lyophilized and analyzed for glutamate quantification.

Synaptosomes were prepared from hypothalami from five CPE-KO and five WT mice littermates (25–35 weeks) by homogenization with 320 mM Sucrose/4 mM HEPES/0.1% bovine serum albumin buffer (SHB) supplemented with complete proteinase inhibitors (Roche, Indianapolis, IN, USA). The homogenate underwent differential centrifugations to obtain synaptosomes as described by Huttner *et al.* (1983). The synaptosomes were suspended with basal buffer and divided equally into five tubes. Activity-dependent secretion was preformed by incubating two tubes of synaptosomes with basal buffer for 10 min while the other two were incubated for 10 min in stimulation buffer. Then the buffers were collected by centrifugation at 1000 *g* for 5 min, and the supernatants were lyophilized for glutamate quantification. The synaptosomes in the fifth tube were used for total glutamate measurement without the secretion assay. Three independent experiments were carried out for this study.

Glutamate quantification

Glutamate measurement using HPLC was conducted in the Amino Acid Laboratory of the Department of Pediatrics, Indiana University

Medical School, as described previously (Battaglia *et al.* 1999) with modifications. Briefly, samples were reconstituted with internal standard solution and dried. The sample was then treated with derivative solution, and separated by reverse-phase HPLC, using a Waters PICO Tag column (Waters, Milford, MA, USA) and propriety buffers. The concentration of glutamate in the samples was quantified against the standard curve and expressed as nmol/mL. For comparison between the study groups, the percentage of glutamate secretion was obtained by dividing the amount of glutamate in the buffers with total glutamate obtained from the cultured neurons or synaptosomes and expressed as % ±SE of total. Student's *t*-test was used to evaluate statistically significant differences. p-Value < 0.05 was considered significantly different.

Electron microscopy (EM)

Four hypothalami from CPE-KO mice and four WT littermates (40–45 weeks) were fixed in 2.5% glutaraldehyde made up in Molling's solution. Transmission electron microscopy was preformed by JFE Enterprises (Brookeville, MD, USA). The electronic micrograph images for 100 synaptic junctions from each group were analyzed using 'Metamorph' software (Molecular Devices Corp., Palo Alto, CA, USA). First, the total number of the SVs in the pre-synaptic terminals was counted for 40 boutons in each group. Next, the docked SVs (defined as no space between vesicle and the pre-synaptic membrane aligned with the post-synaptic density) and the number of SVs within the pre-active zone [100 nm from the pre-synaptic membrane (depth) × entire region aligned with the post-synaptic density (length)] were analyzed for 40 synapses from each group. In addition, the average densities of SVs per 100 nm × 100 nm between 0–100, 100–200, 200–300, and 300–400 nm from the pre-synaptic membrane were calculated from 26 boutons of CPE-KO mice and WT littermates using Metamorph.

Immunoprecipitation assay for intact Svs

To examine whether SVs have the cytoplasmic tail of CPE on the outside surface, ten hypothalami of adult Sprague Dawley rats (25 weeks) were utilized to obtain crude synaptosomes. The synaptosomes underwent hypotonic lysis in 32 mM sucrose buffer with homogenization, differential centrifugation, and ultracentrifugation to isolate SVs (Huttner *et al.* 1983). Aliquots of the hypothalamic lysate, synaptosomes, and the purified SVs were analyzed by Western blotting.

For immunoprecipitation assays, an affinity-purified rabbit antibody against the 10 amino acid residues at the extreme CPE-C-terminus (anti-CPE_{C10} or C-CPE) was covalently coupled to the linker bound magnetic Dynabeads M-500 subcellular beads (Invitrogen, Carlsbad, CA, USA) specialized for pull down of intact vesicles following the manufacturer's instruction. Intact SVs (100 μL) were incubated with these beads (4×10^7) overnight at 4°C and gentle rotation. To determine the specificity of CPE binding, the same volume of the SVs were incubated with two controls: one with C-CPE coupled Dynabeads that were pre-incubated with 8 μg of the CPE_{C10} peptide (C-CPE + peptide), and the other with only the linker IgG bound Dynabeads (IgG). Following the incubation, the Dynabeads were washed and the bound proteins were eluted with sample buffer at 95°C for 5 min and analyzed by Western blot.

To examine whether the SVs were structurally intact, we coupled Dynabeads with an antibody against an internal sequence of CPE (I-CPE, aa362–379); a sequence that is expected to reside inside the synaptic vesicle. These Dynabeads were incubated with same amount of intact SVs or lysed vesicles (with three freeze-thaw cycles). The Dynabeads with linker IgG and C-CPE were used in parallel as controls. Three independent experiments were carried out for these studies.

Immunoprecipitation assay for PC12 cell was done with the combined fractions of 5–8, which contains enriched SLMVs after the subcellular fractionation by sucrose density gradient centrifugation.

Co-precipitation study using GST-CPE_{C10}

To determine the CPE-C terminal interactive proteins, CPE cytoplasmic terminal 10 residues tagged with GST (GST-CPE_{C10}) was made and co-precipitation studies using GST or GST-CPE_{C10} with mouse brain and PC12 cell cytosols were performed as described previously (Park *et al.* 2008a). The interactive proteins in the pull-down fractions were analyzed by Western blot.

Sucrose density gradient fractionation of hypothalamic SVs

Synaptic vesicles isolated from mouse brain were further analyzed by sucrose gradient velocity centrifugation. The SVs were layered on the top of a 50–800 mM sucrose gradient generated with a Gradient Master (BIO MP, Canada) and centrifuged for 5 h at 65 000 *g*. Sixteen 1 mL fractions were collected from the top of the gradient using the Auto Densi Flow fraction collector (Labconco, Kansas City, MO, USA). To determine whether the CPE present in the synaptic vesicle fractions was a contaminant from the homogenization process, exogenous CPE was added to synaptosomes of CPE-KO mice before hypotonic lysis. The exogenous CPE was obtained from conditioned medium of COS7 cells transduced with an adenovirus expressing full-length CPE. Sixteen fractions were collected after centrifugation and proteins in each fraction were precipitated with 10% trichloroacetic acid. The presence of CPE and synaptic vesicle markers were determined by Western blot.

For the analysis of PC12 cell SLMVs, cells grown in four 100 mm dishes were harvested using trypsin, washed, and suspended in 1 mL of 32 mM SHB buffer. The cells were homogenized by passage through 20G and 27G needles 10 times each, and centrifuged at 1000 *g* to remove cell debris. The post-nuclear supernatant was then fractionated by sucrose gradient centrifugation and 17 fractions were collected and analyzed by Western blot as described above for the hypothalamic SVs.

Western blotting and antibodies

Quantification of proteins in the cell or tissues was preformed by Western blotting. Proteins were separated on 4–12% NuPage (Invitrogen) and transferred onto nitrocellulose or polyvinylidene difluoride membrane for immunoblotting. The rabbit antibody against the 10 residues at the CPE carboxyl terminus (Normant and Loh 1998) and the internal control CPE antibody (aa362–379) made in our laboratory were used for immunoprecipitation and immunoblotting. For detection of Rab27A, Rab3A, and Rim1, and DIC, horseradish peroxidase-conjugated secondary antibodies and the ECL plus Western Blotting Detection System (GE Healthcare, Piscataway, NJ, USA) were used. To detect CPE, chromogranin A, Syn, synapsin1, vesicular glutamate transporter (VGLUT) 1, VGLUT 2, and vesicle-associated membrane protein 2 (VAMP 2),

IRDye™ conjugated secondary antibodies (Rockland Immunochemicals, Gilbertsville, PA, USA) were used and the fluorescent signals were analyzed by the Odyssey Infrared Imager System (LI-COR, Inc., Lincoln, NE, USA). The fluorescence intensities of corresponding bands were recorded as mean ± SE of arbitrary units from at least three separate experiments. Detailed information for antibodies used in the Western blotting is in Appendix S1.

TIRF microscopy

To evaluate the distribution of SLMVs in the TIRF zone (~200 nm from the plasma membrane), 2×10^4 PC12 cells were seeded onto 0.17 mm delta TPG dish coated with 0.001% poly-lysine and poly-ornithine, and incubated for 18 h in Dulbecco's modified Eagle's medium supplemented with 5% horse and 10% fetal bovine sera. The cells were co-transfected with Syn-mRFP and GFP or GFP-tagged CPE cytoplasmic tail (GFP-CPE_{C15}) for 24 h using Lipofectamine 2000 (Invitrogen). The medium was replaced with basal TIRF buffer (Michael *et al.* 2007) and the steady-state distribution of fluorescent proteins in the TIRF zone were captured with an inverted Olympus IX81 microscope (Olympus, Center Valley, PA, USA). The microscope was equipped with a 60× PlanApo-N 1.45 NA, oil objective and a Hamamatsu Orca C9100 backed-thinned camera (electron multiplying charge-coupled device) with 512 × 512 pixels. The charge-coupled device detector gain was fixed at 250 for all the images of cells. The temperature of the stage was heated to 37°C before dish mounting. The GFP signals were also observed under epi-fluorescence microscopy, and the average intensity of Syn-mRFP was measured with 'Metamorph' software for each group and expressed as arbitrary units. Two independent experiments were performed for this measurement. Details of signal-to-noise ratio determination for TIRF are described in Appendix S1.

Yeast two-hybrid library screen

Mouse brain cDNA library in pACT2-1 (ML4008AH; *LEU*$^+$) were purchased from Clontech (Mountain View, CA, USA). cDNA encoding the C-terminal 25 amino acids of C-terminal 25 amino acids of CPE (CPE_{C25}) was subcloned into the *Eco*RI and *Pst*I sites of the yeast two-hybrid bait plasmid pAS2-1 (Clontech). The construct was confirmed by sequencing. Of cDNAs from 1×10^7 independent clones, 10% of the brain library was screened. Positive cDNAs were purified, sequenced and then subjected to a homology search via NCBI BLAST.

Results

Activity-dependent glutamate secretion is impaired in the hypothalamic neurons of CPE-KO mice

To determine if CPE is involved in neurotransmitter release, we examined the regulated secretion of glutamate, a major neurotransmitter in the hypothalamus, using primary embryonic neurons in culture. Embryonic neurons isolated from WT or CPE-KO mice were incubated with either basal or stimulation buffer and the secretion of glutamate in the buffer was quantified (Fig. 1a). There was no significant K^+-induced secretion of glutamate from the neurons of CPE-KO mice [basal secretion (4.1 ± 0.4%) vs. stimulated secretion (6.3 ± 0.8%), $p > 0.05$] while a significant stimulated secretion of glutamate from the WT hypothalamic neurons was observed [basal secretion (4.4 ± 0.7%) vs. stimulated secretion (11.33 ± 3.0%), $p < 0.02$]. To examine whether the reduction of glutamate secretion was because of a decrease in glutamate content in CPE-KO neurons compared with WT, we quantified the total amount of glutamate in these neurons, and found that there was no significant difference (CPE-KO, 99 ± 12 nmol/mL; WT, 115 ± 11 nmol/mL, $p > 0.05$; Fig. 1b).

The glutamate secretion in adult hypothalamic synaptosomes was also examined with synaptosomes isolated from CPE-KO or WT mouse hypothalami. In WT synaptosomes, the percentage of glutamate secretion was significantly higher in the stimulated media (40.2 ± 8.7%) than that of basal medium (22.2 ± 3.7%, $p < 0.05$) while it was not significantly different between basal and stimulated media in CPE-KO mouse synaptosomes (28.6 ± 5.7% vs. 29.8 ± 7.3%, respectively, $p > 0.05$; Fig. 1c). The total amount of glutamate in the synaptosomes was not significantly different between CPE-KO (91 ± 14 nmol/mL) and WT mice (80 ± 15 nmol/mL,

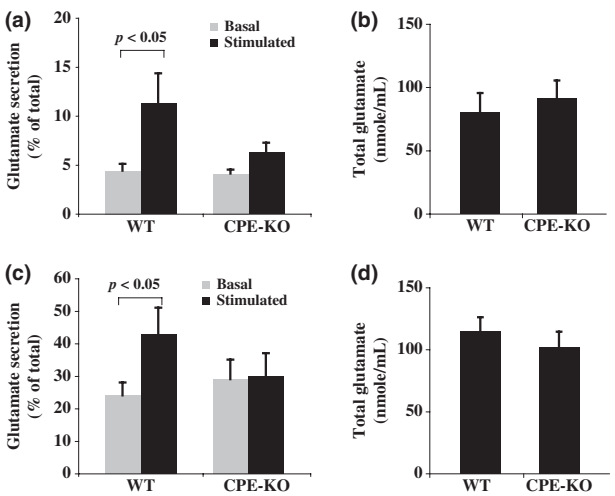

Fig. 1 Analysis of K^+-stimulated glutamate secretion from hypothalamic neurons and synaptosomes. (a) Glutamate secretion [% = glutamate in medium divided by total glutamate ± SEM × 100%] from primary hypothalamic neurons ($N = 3$). Hypothalamic neurons derived from wild type (WT, $N = 10$) or carboxypeptidase E knockout (CPE-KO; $N = 10$) E16 mouse hypothalami were treated in basal buffer or 50 mM KCl-containing stimulation buffer for 10 min. The glutamate levels in the basal and stimulation buffers and in the cells were quantified by HPLC against a standard curve and expressed as nmol/mL. The basal level of glutamate secreted was similar in both groups; but stimulated glutamate secretion was significantly higher in WT hypothalamic neurons than that of CPE-KO mice ($p < 0.05$). (c) The percentage of stimulated glutamate secretion by synaptosomes isolated from adult hypothalami of WT and CPE-KO mice ($N = 3$). The total glutamate content was not significantly different between WT and CPE-KO embryonic hypothalamic neurons (b) or adult hypothalamic synaptosomes (d) ($N = 3$).

$p > 0.05$; Fig. 1d). These results suggest that CPE is involved, either directly or indirectly, in activity-dependent glutamate secretion from hypothalamic neurons.

The number of SVs in the active and pre-active zones at the pre-synaptic membrane is reduced in hypothalamic synapses of CPE-KO mice

To examine whether CPE-KO mouse hypothalami have a normal distribution of SVs accumulated at the pre-synaptic membrane, we examined the hypothalamic synaptic junctions of WT and CPE-KO mice by electron microscopy (Fig. 2a–d). We first analyzed the total number of SVs in 40 boutons from each group and found that there was no significant difference between animals (WT; 195.6 ± 8.4/bouton and CPE-KO; 192.5 ± 8.5/bouton, $p > 0.2$). Next, we found that 39.8 ± 2.1% of the CPE-KO synapses ($N = 123$) lacked tethered/docked SVs at active zone of the pre-synaptic membrane in contrast to that of 14.2 ± 2.0% of

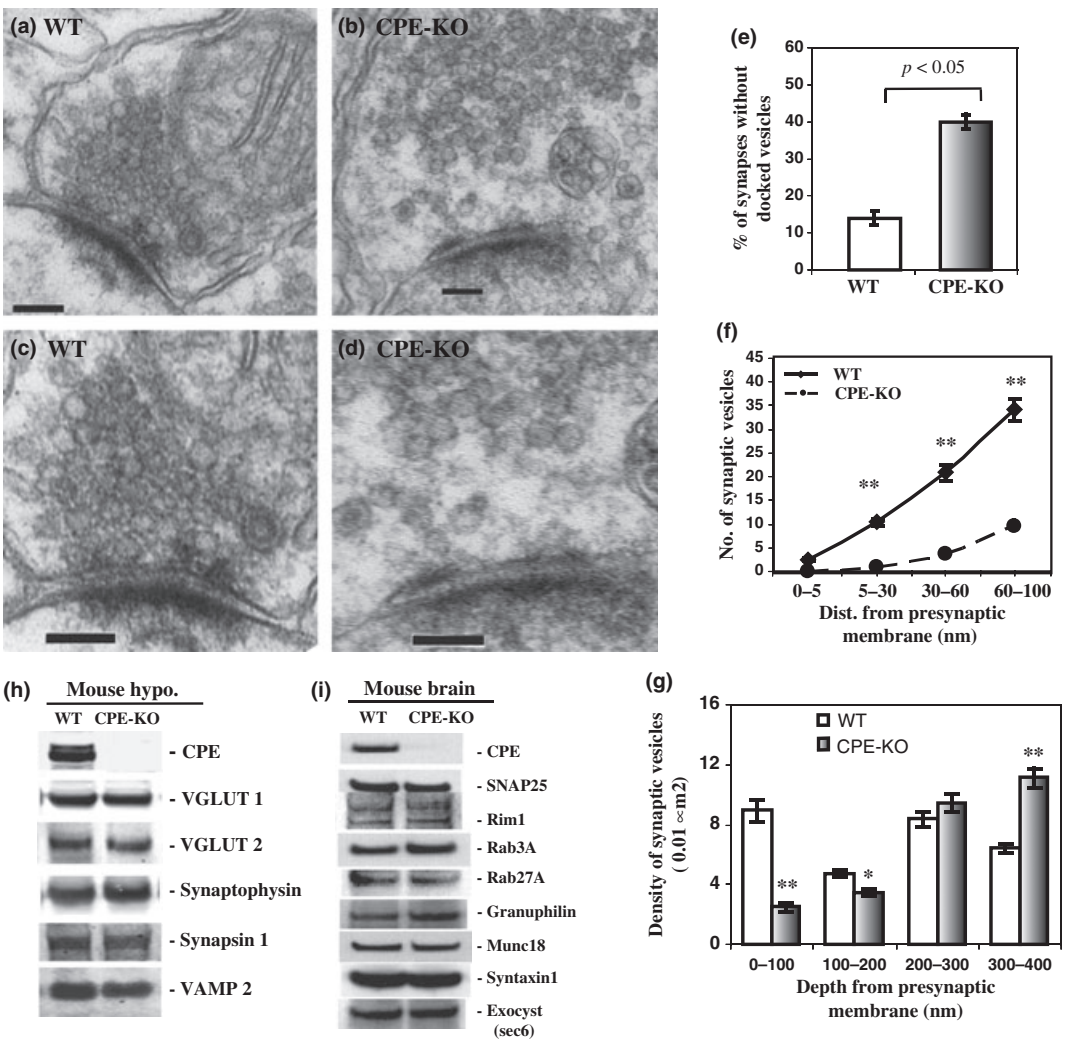

Fig. 2 Comparison of hypothalamic synapse morphology between wild type (WT) and carboxypeptidase E knockout (CPE-KO) mice. Representative electronic micrograph (EM) of hypothalamic synapses from WT (a) and CPE-KO mice (b) (Scale bar = 100 nm). Magnified EM images of hypothalamic synapses from WT (c) and CPE-KO (d) mice (Scale bar = 100 nm). (e) Bar graph showing the percentage of synapses without tethered/docked synaptic vesicles (SVs) at active zone of the pre-synaptic membrane in the hypothalami of CPE-KO mice ($N = 123$) was significantly higher than that of their WT littermates ($N = 134$). (f) Line graph showing the number of SVs within the zone 5, 30, 60, 100 nm away from the pre-synaptic membrane (depth) and entire area along the post-synaptic density (width) of the CPE-KO ($N = 40$) and WT mouse synapses ($N = 40$). (g) The average density of SVs per 100 nm × 100 nm (0.01 μm^2) between 0–100, 100–200, 200–300, and 300–400 nm from the pre-synaptic membrane from 26 boutons of CPE-KO mice and WT littermates. $^*p < 0.05$; $^{**}p < 0.0002$. (h) Representative Western blot showing the levels of proteins associated with synaptic vesicle in the hypothalamus (Hypo.) of CPE knock out (KO) mouse or their wild-type littermates (WT). (i) Immunoblots demonstrate the levels of proteins related with synaptic vesicle tethering/docking in the brain cytosol of CPE-KO mouse or their wild-type littermates (WT). All experiments were repeated three times with similar results.

the WT synapses (N = 134; Fig. 2e). Finally, by analyzing 40 synapses from each group, we found that the number of SVs localized 5, 30, 60, and 100 nm from the pre-synaptic membrane was significantly reduced in the CPE-KO synapses compared with those of WT (all: $p < 0.0002$, Fig. 2f). These results indicate that the absence of CPE results in the lack of localization of SVs in the active and pre-active zone of hypothalamic synapses.

We also determined the density of SVs per 100 nm × 100 nm (0.01 μm^2) between 0–100, 100–200, 200–300, and 300–400 nm from the pre-synaptic membrane from 26 boutons of CPE-KO mice and WT littermates. The density of SVs was lower in the hypothalamic boutons of CPE-KO mice compared with WT mice up to 200 nm from the pre-synaptic membrane (Fig. 2g). Thereafter, the SV density of CPE-KO mice was similar to that of WT mice between 200 and 300 nm, and was slightly higher in CPE-KO versus WT mice between 300 and 400 nm. The data indicate that SVs absent below 200 nm (pre-active zone) were retained in the pool above 300 nm from the pre-synaptic membrane.

Since it was possible that the KO of one protein might affect the level of other proteins, we examined the levels of several synaptic vesicle-associated proteins from the mouse hypothalamus (Hypo.), such as VGLUT 1 and VGLUT 2, synapsin 1, VAMP 2 (Fig. 2h), as well as other proteins involved in synaptic vesicle tethering or docking, such as Munc18-1, syntaxin1, Rim1, Rab3A, Rab27A, granuphilin, exocyst (Sec6), and SNAP25 (Fig. 2i) in mouse brain. We observed that the levels of these proteins were unchanged in the CPE-KO mouse when compared with their WT littermates. This shows that the lack of SVs in the active zone and in the vicinity of the active zone of the synapses of the CPE-KO mouse is not because of a defect of assembly or integrity of SV, nor lack of known molecules involved in the tethering or docking process.

Hypothalamic SVs contain transmembrane CPE

Synaptic vesicle localization in the active zone at the pre-synaptic membrane is mediated not only by scaffolding proteins but also by vesicle-associated proteins (De Camilli and Jahn 1990; Murthy and De Camilli 2003). We therefore examined SVs isolated from rat hypothalamus for the presence of CPE. We found CPE not only in the heavy peptidergic vesicle fractions as expected (data not shown) but also in the synaptosomes and the purified synaptic vesicle fractions, which were marked by Syn but lacked chromogranin A, a peptidergic vesicle marker (Fig. 3a).

Given that a subpopulation of CPE in peptidergic vesicles has a transmembrane orientation in endocrine cells (Dhanvantari *et al.* 2002; Arnaoutova *et al.* 2003), it is possible that hypothalamic SVs may also have a similar transmembrane form of CPE. To test this hypothesis, we used immunoprecipitation experiments with Dynabeads coupled with an antibody against the last 10 residues of the CPE cytoplasmic tail (anti-CPE$_{C10}$ or C-CPE). The C-CPE did pull down intact SVs isolated from adult rat hypothalami; indicated by the presence of CPE and three SVs markers, Syn, VGLUT2, and VGLUT1 (Fig. 3b). The two controls, pre-absorbed C-CPE with CPE$_{C10}$ peptide (C-CPE + peptide) and the Dynabeads cross-linked to a non-specific IgG

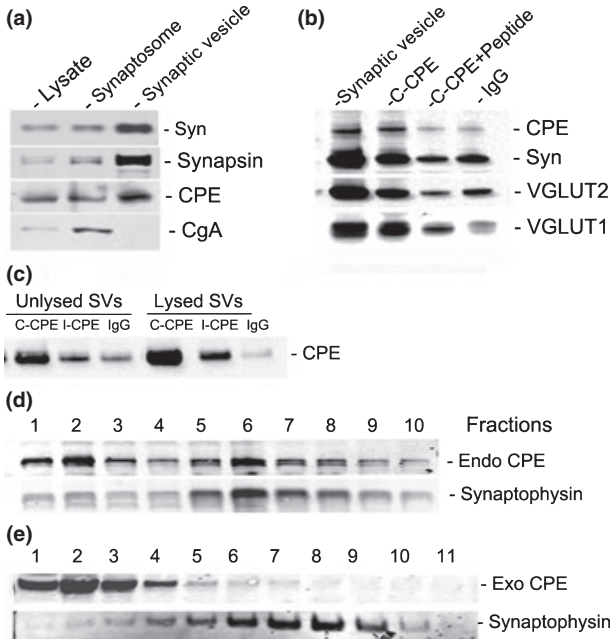

Fig. 3 Proteins in synaptic vesicles (SVs) isolated from rat hypothalamus and mouse brain. (a) Representative Western blots of hypothalamic lysate (Lysate), synaptosomes, and purified SVs from adult rat hypothalamus. The presence of carboxypeptidase E (CPE) was evident in all the fractions, including SVs which were positive for two SV markers, synaptophysin (Syn), and synapsin, while chromogranin A, a marker for dense-core secretory granules, was absent in the SV fraction. (b) Representative Western blot of intact SVs that were immunoprecipitated (IP) by Dynabeads coupled with anti-CPE$_{C10}$ antibody (C-CPE) indicated by strong activity to anti-vesicular glutamate transporter (VGLUT)1, VGLUT2, and synaptophysin (Syn) antibodies. Two controls were used to demonstrate the specificity of anti-CPE$_{C10}$ antibody: the C-CPE beads pre-absorbed with CPE$_{C10}$ peptide before the IP (C-CPE + peptide), and beads that only had linker IgG (IgG). The immunoreactivity to CPE and all the SV markers were eliminated by the absorption control peptide. (c) IP assay using the anti-CPE internal sequences (I-CPE) antibody with intact or lysed SVs. C-CPE or IgG coupled to Dynabeads was used as positive and negative controls. I-CPE only precipitated the CPE when the vesicles were lysed (Lysed SV) (N = 3). (d) SVs isolated from WT mouse brain were analyzed by Western blot after fractionation by sucrose gradient centrifugation. Immunoreactivity of endogenous CPE was observed in fractions containing synaptophysin (fractions 5–8). (e) Western blot of SV fractions after the sucrose gradient for CPE-KO mouse brain. The SVs were prepared in the presence of exogenous full-length CPE. This exogenous CPE was present in the first four fractions but not detected in fractions containing synaptophysin (Fractions 5–9).

(IgG), pulled down only background levels of SVs (Fig. 3b). These results indicate that hypothalamic SVs contain a transmembrane form of CPE that exposes its C-terminus to the cytoplasm.

To rule out the possibility that the presence of CPE in the SVs might be due to binding of soluble CPE released from lysed peptidergic vesicles during homogenization, we performed two additional control experiments. First, we incubated Dynabeads coupled with an antibody against an internal CPE sequence (I-CPE, aa 362–379: present inside SVs) with either intact SVs or lysed SVs in parallel. We found that the I-CPE antibody pulled down a small amount of CPE from the unlysed SVs (Fig. 3c, left panel) with a significant increase in the amount of CPE from lysed SVs (2.5 ± 0.3-fold, $n = 3$, $p < 0.02$; Fig. 3c, right panel). The intensity of CPE in the lysed samples precipitated by C-CPE also increased significantly compared with unlysed vesicles (2.4 ± 0.02-fold, $n = 3$, $p < 0.02$). These results strongly suggest that the SVs used in the previous experiments (Fig. 3a and b) were for the most part structurally intact and that no significant amount of full-length CPE was bound to the outside of the SVs. As a second control experiment, we examined whether exogenous soluble CPE could be co-fractionated with intact SVs. We examined the distribution of CPE in the SVs isolated from WT and CPE-KO mouse brains by subcellular fractionation and Western blot. In fractions of WT mouse brain, but not the CPE-KO, we found CPE in SV fractions (5–9), which also contained Syn, the synaptic vesicle marker (Fig. 3d). Next, we repeated the purification of SVs from CPE-KO mice but this time we added conditioned medium containing full-length soluble CPE expressed in COS7 cells, to the synaptosomes before the hypotonic lysis procedure. The conditioned medium from control COS7 cells devoid of CPE was used as control medium added to the synaptosomes in a parallel experiment. We observed that the exogenous CPE did not adhere to the outside of the vesicles, since it was not present in the same fractions as the SVs from WT mouse (fractions 5–9; Fig. 3e). These data indicate that CPE detected in the intact WT SVs was not because of an artifact of adherence of soluble CPE released from damaged vesicles during the homogenization procedure.

Excessive CPE cytoplasmic tail decreases the steady-state accumulation of SLMVs beneath the plasma membrane of PC12 cells

PC12 cells contain SLMVs as a counterpart of SVs and presumably contain a transmembrane form of CPE since chromaffin granules do. Analysis of PC12 cells by subcellular fractionation showed that CPE co-fractionated not only with LDCVs (fractions 14–17, Fig. 4a), but also in some of the Syn-positive SLMV fractions (fractions 4–8; Fig. 4a). We then examined whether the CPE-containing SLMVs have a CPE cytoplasmic tail by the same method used to immunoprecipitate hypothalamic SVs. The anti-CPE_{C10} antibody-coupled Dynabeads pulled down intact SLMVs, as indicated by the presence of CPE and Syn in the eluted fraction (Fig. 4b). The control Dynabeads with linker IgG (IgG) did not pull down SLMVs and CPE-tail peptide (C-pep) pre-absorbed C-CPE-Dynabeads significantly reduced binding (Fig. 4b).

Total internal reflective fluorescence microscopy was used for the acquisition of fluorescence signal within 200 nm underneath the plasma membrane; the focal plane for the TIRF signal or TIRF zone (Steyer *et al.* 1997). If the presence of excessive CPE-tail peptides interferes with the localization of the SLMVs containing Syn-mRFP in the active zone in a dominant negative manner, the intensity of Syn-mRFP within the TIRF zone is expected to be reduced. Using co-transfection and TIRF microscopy, we observed that PC12 cells expressing GFP-CPE_{C15} showed a significant decrease (by 1.96-fold, $n = 20$, $p < 0.005$) in the average intensity of the Syn-mRFP signal within the TIRF zone compared with that in the cells expressing the GFP tag alone (Fig. 4c and d). The decrease was not because of an overall reduction in the expression of Syn-mRFP since the intensity of Syn-mRFP observed under epi-fluorescence microscopy was not different between GFP- and GFP-CPE_{C15}-expressing cells (data not shown). This reduced amount of signal within the TIRF zone implies that the excessive CPE-tail peptides decreased the accumulation of Syn-mRFP-containing SLMVs within 200 nm from the plasma membrane.

CPE cytoplasmic tail interacts with γ-adducin

Based on the findings that the cytoplasmic tail of CPE on peptidergic vesicles in hippocampal neurons and pituitary cells interacts with cytoplasmic machinery for vesicle transport (Park *et al.* 2008a,b), we hypothesized that the CPE-tail might bind to molecule(s) involved in recruiting the vesicle into the pre-active zone at the pre-synaptic membrane.

To identify a CPE-tail-interacting molecule that may be involved in SV localization to the pre-active zone, we conducted a yeast two-hybrid screen of a mouse brain cDNA library using the CPE_{C25} as bait. We found that CPE_{C25} interacted with γ-adducin (Katagiri *et al.* 1996), an isoform of the adducins, F-actin interacting proteins present close to the plasma membrane (Kuhlman *et al.* 1996) (data not shown). Our pull-down experiment using GST-tagged CPE_{C10} (GST-CPE_{C10}) confirmed the interaction between CPE_{C10} and γ-adducin in the cytosol prepared from mouse brain or PC12 cells (Fig. 5a). In addition to γ-adducin, actin was also detected in the GST-CPE_{C10} pull-down fractions from mouse brain (Fig. 5a, left panel), reflecting its interaction with γ-adducin as a complex. In addition, CPE cytoplasmic tail interacted with Rab27A and Rim1, proteins involved in vesicle tethering to the plasma membrane (Wang *et al.* 1997; Tsuboi and Fukuda 2006) while not with the

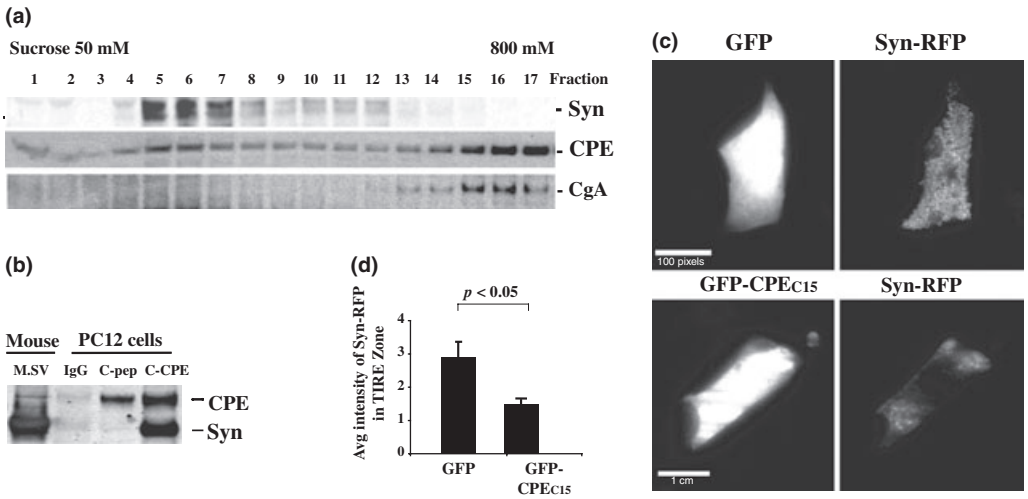

Fig. 4 Analysis of carboxypeptidase E (CPE) in synaptic-like microvesicles (SLMVs) in PC12 cells. (a) Western blot analysis of PC12 cell cytosol fractions after sucrose gradient centrifugation. CPE was present in SLMV fractions (4–8) marked by synaptophysin (Syn), as well as in the fractions (14–17) containing peptidergic vesicles, marked by chromogranin A (a large dense-core vesicle marker). (b) Western blot after pulldown experiment for SLMVs from PC12 cell cytosol using Dynabeads coupled C-CPE antibody, control IgG, or CPE_{C10} peptide pre-absorbed C-CPE (C-pep). SLMVs were pulled down by the CPE_{C10} antibody while the CPE_{C10} peptide absorption control reduced this binding. (c) Analysis of the intensity of synaptophysin-mRFP (Syn-mRFP) within 200 nm (TIRF zone) in PC12 cells (left panels: green epi-fluorescence and right panel: red TIRF). High intensity of Syn-mRFP signal within the TIRF zone showed in cells co-transfected with GFP-vector (upper panel) but not in the GFP-CPE_{C15}-transfected cells (lower panel). Scale bar = 16.6 mm. (d) Bar graph showing the normalized average intensity (arbitrary units ± SEM) of Syn-mRFP in the TIRF zone of the cells expressing either GFP ($N = 20$) or GFP-CPE_{C15} ($N = 20$), $p < 0.005$.

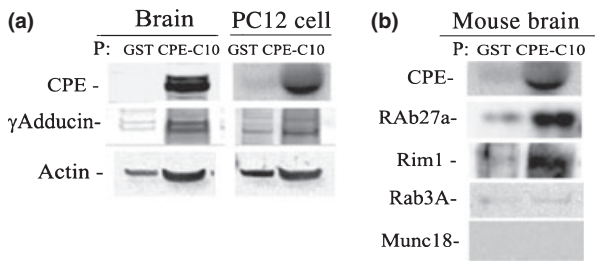

Fig. 5 Detection of levels of proteins associated with synaptic vesicles by western blot. (a) The interactive proteins pulled down by GST-tagged carboxypeptidase (CPE)-tail peptide (GST-CPE_{C10}) or GST controls in wild-type mouse brain or PC12 cell cytosol. In GST-CPE_{C10} pulled down samples, reactivity were shown with γ-adducin and actin antibodies in mouse brain cytosol (left panel) and in PC12 cell cytosol (right panel). (b) Western blot showing Rim1 and Rab27A, but not Rab3A or Munc18, were pulled down by GST-CPE_{C10} in mouse brain. All experiments were repeated twice with similar results.

Rab27A interactor, Munc18-1, and the Rim1 interactor, Rab3A (Fig. 5b). The interaction of CPE-tail with Rim1 was also seen in our yeast two-hybrid screening of a rat brain cDNA library, in which the N-terminus of Rim1 (28–226) which contains the Zn finger and its highly charged region, but not the Rab3A-binding region, interacted with the CPE-C-terminal domain, starting from amino acids 164–209 of CPE and extending to its C-terminus (12 of 116 positive colonies).

Discussion

The existence of SV populations in the pre-synaptic terminal is critical for regulated release of neurotransmitters. In this study, the role of CPE in glutamate release and the localization of SVs in the synaptic pre-active zone were examined in mouse hypothalamic neurons. We focused on vesicles in the hypothalamus, an area of the brain highly enriched in glutamate vesicles as well as peptidergic vesicles.

Our observation of defective glutamate secretion in CPE-KO mouse hypothalamic neurons and adult synaptosomes (Fig. 1) and previous findings of glutamate dependent defects in CPE-KO electroretinograms of the photoreceptors (Zhu *et al.* 2005) indicate a functional role of CPE in neurotransmitter secretion. In addition, deletion of Egl-21, a CPE ortholog in *C. elegans*, resulted in defective acetylcholine secretion from the neuromuscular junction (Jacob and Kaplan 2003) suggesting that the role of CPE in neurotransmitter secretion is functionally conserved across evolution. However, previous proteomic analyses of SVs isolated from whole brain have not reported the presence of CPE in these organelles (Takamori *et al.* 2006). Here, we demonstrated that SVs from hypothalamic neurons and also SLMVs in

PC12 cells contain CPE and that some of these molecules are oriented in a transmembrane manner. When we analyzed SVs from the rest of the brain without the hypothalamus, we did not observe a significant amount of CPE in the SV fractions (data not shown) suggesting that the SVs containing CPE are present primarily in hypothalamic neurons compared with other parts of the brain.

Classical neurotransmitter vesicles co-exist with large dense-core peptidergic vesicles in neuroendocrine neurons (Hrabovszky and Liposits 2008). The presence of CPE in these classical neurotransmitter vesicles, in CPE-rich peptidergic neurons, is perhaps not so surprising since SVs are generated through recycling by endocytosis. This would allow recruitment of CPE from the pre-synaptic membrane deposited there by exocytosis of peptidergic vesicles. Indeed, it has been shown that residual peptidergic cargo from endocrine cells, such as CPE, that remains on the outside of the plasma membrane after exocytosis can be internalized and recycled back to the TGN for possible re-use in another round of granule biogenesis (Arnaoutova *et al.* 2003; Ferraro *et al.* 2005). We predict that general classical neurotransmitter release would not be expected to be severely impaired in the CPE-KO mice except in a subpopulation of hypothalamic neurons; although CPE in SVs in minor populations of peptidergic neurons distributed in other parts of the brain may also exist.

As a means to understand the lack of activity-dependent glutamate secretion in the CPE-KO hypothalamic neurons and adult synaptosomes, we analyzed the hypothalamus at the ultrastructural level by EM. Our analysis showed that there was a significant decrease in the number of SVs in the pre-active zone within 200 nm from the pre-synaptic membrane (Fig. 2). Given the observations that there was (i) no decrease of overall vesicle numbers in the pre-synaptic boutons, (ii) no reduction in total glutamate levels (Fig. 1b and d), and (iii) no changes in the protein levels of VGLUT 1 and VGLUT 2, Syn, VAMP 2, and other SV associated molecules in the CPE-KO mouse hypothalamus when compared with their WT littermates (Fig. 2h and i); it is unlikely that the diminished glutamate release is because of a structural defect in these SVs or a failure in the uptake or storage of glutamate. We speculate that the absence of CPE does not affect SV biogenesis and/or degradation, but causes a preferential loss of SVs accumulated within the pre-active zone.

If CPE is directly involved in the localization of SVs within the pre-active zone, as the static steady-state EM micrographs would indicate, it would have to interact with other proteins. Our yeast two-hybrid study demonstrated that the CPE_{C25} interacted with γ-adducin, an interaction that was recapitulated in GST-CPE_{C10} pull-down experiments using mouse brain and PC12 cell cytosol (Fig. 5a). These results suggest that the CPE cytoplasmic tail on these vesicles can act as a linker to γ-adducin. γ-Adducin is a member of the adducin family (Kuhlman *et al.* 1996), which has traditionally been regarded as a critical component of the cell cytoskeleton since it binds and stabilizes the barbed end of F-actin as well as spectrin, and its rich in the pre-synaptic terminals and structurally stabilizes the terminals (Pielage *et al.* 2005). Our pull-down experiment also detected actin in the precipitated fraction (Fig. 5a). This was expected since F-actins are likely brought down by the GST-CPE_{C10} through interaction with γ-adducin. Hence, we propose that CPE cytoplasmic tail interacts with γ-adducin and actin in the pre-synaptic terminal to facilitate the localization of SVs to the pre-active zone, although the exact mechanism is unclear. Interestingly, in synapsin I KO mice, SVs were also dramatically reduced in the region > 150 nm from the active zone (Li *et al.* 1995; Takei *et al.* 1995) and synapsin IIa was shown to be the primary molecule regulating the reserve pool of glutamatergic SVs in hippocampal neurons (Gitler *et al.* 2008). Mechanistically, synapsin functions in the regulation of SV availability for release by interweaving SVs within the F-actin network at the pre-synaptic terminal (Bloom *et al.* 2003; Siksou *et al.* 2007). Whether the CPE cytoplasmic tail's direct interaction with γ-adducin which then interacts with F-actin works in conjunction with synapsin, or independently to localize SVs to the pre-active zone remains to be determined. We also observed the interaction of GST-CPE_{C10} with Rab27A and Rim1 (Fig. 5b) but not with their binding partners, Munc18-1 and Rab3A, respectively, suggesting that the CPE-tail also interacts with vesicle tethering machinery.

Our yeast two-hybrid, immunoprecipitation, and GST pull down results all indicate that some CPE in these vesicles have a transmembrane orientation, thus exposing its C-terminal tail in the cytoplasm where it can interact with proteins such as γ-adducin to facilitate vesicle localization within the F-actin-rich nerve terminal. To explore this further, we co-expressed the CPE_{C15} tail in PC12 cells with Syn-mRFP and used TIRF microscopy to quantify the signal representing SLMVs within 200 nm from the plasma membrane. Our TIRF experiments showed that at steady-state, the signal of Syn-mRFP in the CPE_{C15} expressing cells was significantly reduced within the TIRF zone compared with the control cells, although overall cellular staining was similar. This provides strong physiological evidence that the CPE-tail is involved in the steady-state localization of SLMVs, a PC12 cell counterpart of SVs, to the F-actin-rich cortex under the plasma membrane to facilitate neurotransmitter release. Based on PC12 cells as a model system, we can interpret that in the absence of CPE, the loss of the interaction of SVs with the F-actin interacting protein γ-adducin could account for the lack of SVs in the pre-active zone area in the CPE-KO hypothalamic neurons. Such a CPE-tail-based mechanism may be limited to neurons expressing abundant amounts of neuropeptides and CPE, and have peptidergic and classical neurotransmitter CPE-

containing vesicles, as in the hypothalamus. While our data favor a physical interaction of the CPE cytoplasmic tail with components of the cytoskeleton at the nerve terminals as a mechanism for lack of localization of SVs in the pre-active zone, leading to impaired glutamate secretion, the possibility that the lack of a neuropeptide, as a result of impaired release of peptidergic vesicles, could cause the observed phenotype and cannot be completely ruled out.

In summary, our current findings indicate that glutamatergic and acetylcholine SVs in the hypothalamus and chromaffin cell-derived PC12 cells, respectively, employ the transmembrane CPE cytoplasmic tail to interact with γ-adducin for recruiting SVs to the active and/or pre-active zone to facilitate neurotransmitter release. This study provides a new insight into the machinery that mediates localization of SVs to the pre-active zone and identifies CPE as a new mediator in this process, hence establishing yet another novel non-enzymatic role of this molecule in the control of classical neurotransmitter release in specific neurons.

Acknowledgements

We thank to laboratory members in SCN, NICHD for technical assistance and helpful discussions. We thank Dr Ronald W. Holz (U. Michgan) for his scientific advice about TIRF microscopy, Dr Leon Lagnado (Cambridge, UK) for Syn-mRFP. We thank Dr Vincent Schram in the NICHD Microscopy Imaging Core for their technical support. Lei Sun was supported by NIH grant RO1 DK050127 to Ronald W. Holz. This research was supported by the Intramural Research Program of the NICHD, NIH. Joshua J. Park has been supported by NICHD K22 and ARRA grants.

Conflict of interest

The authors declare no conflicts of interest.

Supporting information

Additional Supporting Information may be found in the online version of this article:

Appendix S1. Experimental details about antibodies for Western blot and signal-to-noise for TIRF.

As a service to our authors and readers, this journal provides supporting information supplied by the authors. Such materials are peer-reviewed and may be re-organized for online delivery, but are not copy-edited or typeset. Technical support issues arising from supporting information (other than missing files) should be addressed to the authors.

References

Arnaoutova I., Jackson C. L., Al-Awar O. S., Donaldson J. G. and Loh Y. P. (2003) Recycling of Raft-associated prohormone sorting receptor carboxypeptidase E requires interaction with ARF6. *Mol. Biol. Cell* **14**, 4448–4457.

Battaglia A., Bertoluzza A., Calbucci F., Eusebi V., Giorgianni P., Ricci R., Tosi R. and Tugnoli V. (1999) High-performance liquid chromatographic analysis of physiological amino acids in human brain tumors by pre-column derivatization with phenylisothiocyanate. *J. Chromatogr. B Biomed. Sci. Appl.* **730**, 81–93.

Bloom O., Evergren E., Tomilin N., Kjaerulff O., Low P., Brodin L., Pieribone V. A., Greengard P. and Shupliakov O. (2003) Colocalization of synapsin and actin during synaptic vesicle recycling. *J. Cell Biol.* **161**, 737–747.

Cawley N. X., Zhou J., Hill J. M., Abebe D., Romboz S., Yanik T., Rodriguiz R. M., Wetsel W. C. and Loh Y. P. (2004) The carboxypeptidase E knockout mouse exhibits endocrinological and behavioral deficits. *Endocrinology* **145**, 5807–5819.

Cool D. R., Normant E., Shen F., Chen H. C., Pannell L., Zhang Y. and Loh Y. P. (1997) Carboxypeptidase E is a regulated secretory pathway sorting receptor: genetic obliteration leads to endocrine disorders in Cpe(fat) mice. *Cell* **88**, 73–83.

De Camilli P. and Jahn R. (1990) Pathways to regulated exocytosis in neurons. *Annu. Rev. Physiol.* **52**, 625–645.

Dhanvantari S., Arnaoutova I., Snell C. R., Steinbach P. J., Hammond K., Caputo G. A., London E. and Loh Y. P. (2002) Carboxypeptidase E, a prohormone sorting receptor, is anchored to secretory granules via a C-terminal transmembrane insertion. *Biochemistry* **41**, 52–60.

Dieck S., Sanmarti-Vila L., Langnaese K. *et al.* (1998) Bassoon, a novel zinc-finger CAG/glutamine-repeat protein selectively localized at the active zone of presynaptic nerve terminals. *J. Cell Biol.* **142**, 499–509.

Fenster S. D., Chung W. J., Zhai R., Cases-Langhoff C., Voss B., Garner A. M., Kaempf U., Kindler S., Gundelfinger E. D. and Garner C. C. (2000) Piccolo, a presynaptic zinc finger protein structurally related to bassoon. *Neuron* **25**, 203–214.

Ferraro F., Eipper B. A. and Mains R. E. (2005) Retrieval and reuse of pituitary secretory granule proteins. *J. Biol. Chem.* **280**, 25424–25435.

Fricker L. D. and Snyder S. H. (1982) Enkephalin convertase: purification and characterization of a specific enkephalin-synthesizing carboxypeptidase localized to adrenal chromaffin granules. *Proc. Natl Acad. Sci. USA* **79**, 3886–3890.

Fricker L. D., Das B. and Angeletti R. H. (1990) Identification of the pH-dependent membrane anchor of carboxypeptidase E (EC 3.4.17.10). *J. Biol. Chem.* **265**, 2476–2482.

Gitler D., Cheng Q., Greengard P. and Augustine G. J. (2008) Synapsin IIa controls the reserve pool of glutamatergic synaptic vesicles. *J. Neurosci.* **28**, 10835–10843.

Hrabovszky E. and Liposits Z. (2008) Novel aspects of glutamatergic signalling in the neuroendocrine system. *J. Neuroendocrinol.* **20**, 743–751.

Huttner W. B., Schiebler W., Greengard P. and De Camilli P. (1983) Synapsin I (protein I), a nerve terminal-specific phosphoprotein. III. Its association with synaptic vesicles studied in a highly purified synaptic vesicle preparation. *J. Cell Biol.* **96**, 1374–1388.

Jacob T. C. and Kaplan J. M. (2003) The EGL-21 carboxypeptidase E facilitates acetylcholine release at *Caenorhabditis elegans* neuromuscular junctions. *J. Neurosci.* **23**, 2122–2130.

Katagiri T., Ozaki K., Fujiwara T., Shimizu F., Kawai A., Okuno S., Suzuki M., Nakamura Y., Takahashi E. and Hirai Y. (1996) Cloning, expression and chromosome mapping of adducin-like 70 (ADDL), a human cDNA highly homologous to human erythrocyte adducin. *Cytogenet. Cell Genet.* **74**, 90–95.

Kuhlman P. A., Hughes C. A., Bennett V. and Fowler V. M. (1996) A new function for adducin. Calcium/calmodulin-regulated capping of the barbed ends of actin filaments. *J. Biol. Chem.* **271**, 7986–7991.

Li L., Chin L. S., Shupliakov O. *et al.* (1995) Impairment of synaptic vesicle clustering and of synaptic transmission, and increased seizure propensity, in synapsin I-deficient mice. *Proc. Natl Acad. Sci. USA* **92**, 9235–9239.

Lou H., Kim S. K., Zaitsev E., Snell C. R., Lu B. and Loh Y. P. (2005) Sorting and activity-dependent secretion of BDNF require interaction of a specific motif with the sorting receptor carboxypeptidase E. *Neuron* **45**, 245–255.

Lou H., Smith A. M., Coates L. C., Cawley N. X., Loh Y. P. and Birch N. P. (2007) The transmembrane domain of the prohormone convertase PC3: a key motif for targeting to the regulated secretory pathway. *Mol. Cell. Endocrinol.* **267**, 17–25.

Michael D. J., Xiong W., Geng X., Drain P. and Chow R. H. (2007) Human insulin vesicle dynamics during pulsatile secretion. *Diabetes* **56**, 1277–1288.

Murthy V. N. and De Camilli P. (2003) Cell biology of the presynaptic terminal. *Annu. Rev. Neurosci.* **26**, 701–728.

Normant E. and Loh Y. P. (1998) Depletion of carboxypeptidase E, a regulated secretory pathway sorting receptor, causes misrouting and constitutive secretion of proinsulin and proenkephalin, but not chromogranin A. *Endocrinology* **139**, 2137–2145.

Park J. J., Cawley N. X. and Loh Y. P. (2008a) Carboxypeptidase E Cytoplasmic Tail-Driven Vesicle Transport Is Key for Activity-Dependent Secretion of Peptide Hormones. *Mol. Endocrinol.* **22**, 989–1004.

Park J. J., Cawley N. X. and Loh Y. P. (2008b) A bi-directional carboxypeptidase E-driven transport mechanism controls BDNF vesicle homeostasis in hippocampal neurons. *Mol. Cell. Neurosci.* **39**, 63–73.

Pielage J., Fetter R. D. and Davis G. W. (2005) Presynaptic spectrin is essential for synapse stabilization. *Curr. Biol.* **15**, 918–928.

Rizzoli S. O. and Betz W. J. (2005) Synaptic vesicle pools. *Nat. Rev. Neurosci.* **6**, 57–69.

Siksou L., Rostaing P., Lechaire J. P. *et al.* (2007) Three-dimensional architecture of presynaptic terminal cytomatrix. *J. Neurosci.* **27**, 6868–6877.

Steyer J. A., Horstmann H. and Almers W. (1997) Transport, docking and exocytosis of single secretory granules in live chromaffin cells. *Nature* **388**, 474–478.

Takamori S., Holt M., Stenius K. *et al.* (2006) Molecular anatomy of a trafficking organelle. *Cell* **127**, 831–846.

Takei Y., Harada A., Takeda S., Kobayashi K., Terada S., Noda T., Takahashi T. and Hirokawa N. (1995) Synapsin I deficiency results in the structural change in the presynaptic terminals in the murine nervous system. *J. Cell Biol.* **131**, 1789–1800.

Tsuboi T. and Fukuda M. (2006) Rab3A and Rab27A cooperatively regulate the docking step of dense-core vesicle exocytosis in PC12 cells. *J. Cell Sci.* **119**, 2196–2203.

Wang Y., Okamoto M., Schmitz F., Hofmann K. and Sudhof T. C. (1997) Rim is a putative Rab3 effector in regulating synaptic-vesicle fusion. *Nature* **388**, 593–598.

Zhu X., Wu K., Rife L. *et al.* (2005) Carboxypeptidase E is required for normal synaptic transmission from photoreceptors to the inner retina. *J. Neurochem.* **95**, 1351–1362.